Journal of Physical Science and Application 2 (4) (2012) 61-70

A Mathematical Model for Pulsating Flow of Ionic Fluid under an Axial Electric Field: EMF Effect on Blood Flow

Mona A. El-Naggar and Medhat A. Messiery

Engineering Physics and Mathematics Department, Faculty of Engineering, Cairo University, Greater Cairo, Egypt

Received: February 02, 2012 / Accepted: March 05, 2012 / Published: April 15, 2012.

Abstract: The present work introduces a mathematical model for ionic fluid that flows under the effect of both pulsating pressure and axial electromagnetic field. The fluid is treated as a Newtonian fluid applying Navier-Stokes equation. The fluid is considered as a neutral mixture of positive and negative ions. The effect of axial electric field is investigated to determine velocity profiles. Hydroelectric equation of the flow is deduced under dc and ac external electric field. Hence the effect of applied frequency (0-1 GHz) and amplitude (10-350 V/m) is illustrated. The ultimate goal is to approach the problem of EMF field interaction with blood flow. The applied pressure waveform is represented as such to simulate the systolic-diastolic behavior. Simulation was carried out using Maple software using blood plasma parameters; hence velocity profiles under various conditions are reported.

Key words: Newtonian fluid, navier-stokes, ionic fluid, blood flow, electric field, hydroelectric flow, simulation, velocity profiles, EMF bioeffects.

Nomenclature

t:	Time
T:	Periodic time
R:	Radius
c:	Sound velocity
∇p :	The pressure gradient
F:	Body force
F_r:	Radial force
F_r:	Axial force
$f_0(t)$:	Driving force
v_r:	Radial velocity
v_r:	Axial velocity
$v^+(t)$:	Axial velocity when the ionic concentration is ρ_{e+}
$v^-(t)$:	Axial velocity when the ionic concentration is ρ_{e-}
$C^-(t)$:	Capactitance
J_z:	Axial current density
J_r:	Radial current density
E_z :	Axial electric field
E_0 :	Maximum applied electric field
B_θ :	Angular magnetic field
B_0 :	Maximum applied magnetic field
Re:	Reynold's number
S_r:	Power density

Greek Letters

σ:	Electrical conductivity
ρ:	Mass density
η:	Viscosity coefficient
γ	Shear rate
ε	Permittivity of the ionic fluid.
ρ_{e+}:	Positive ionic concentration
ρ_{e-} :	Negative ionic concentration
μ :	Magnetic permeabilitiy

1. Introduction

Recently, hemodynamic properties depend greatly on mathematical analysis of fluid dynamics. Hemodynamic variables are known to impact the genesis of atherosclerosis and formation of thrombosis. It is possible that many cardiovascular diseases can be detected and diagnosed by analyzing the profiles of the velocity components. Being an important field of research for quite a while, various mathematical models have been adopted to reproduce blood velocity profiles in different blood vessels. Navier-Stokes equation is one of the most commonly used analytical methods to study hydromagnetic and hydroelectric

Corresponding author: Mona A. El-Naggar, assistant professor, research fields: biophysics, molecular, atomic physics and electromagnetics. E-mail: monaelnaggar@msn.com.

flow. The equation is applicable as such to produce velocity components of electrically conducting Newtonian fluids subjected to magnetic, electric fields, or both. Blood flow in large arteries, can be analogous to ionic fluid flow in a cylindrical vessel.

The main issue facing scientists and mathematicians while attempting to simulate the flow in blood vessels is that blood flow rheology is complex. The complexity of which arises from the viscosity property that is not only vessel dependent but shear dependent as well. The axial velocity magnitude depends greatly on the wall viscoelastic properties [1], besides the initial distribution of velocity. The wall viscosity affects greatly the shear forces and hence shear rate, whereas the elasticity affects the magnitude of momentum and strain energy relayed to the successive arterial section [2, 3]. However, it is obvious that the blood flow models, introduced mainly to deduce hemodynamic variables, mostly neglect the arterial wall viscoelastic properties. Numerical techniques give different models to predict different results of hemodynamic variables.

One of the major problems in studying the blood flow is that its viscosity varies not only with its speed but also with the diameter of the blood vessel. The current models are far from being comprehensive and lacks consistency hence one can state that the problem lacks general agreement upon a model. However, under the general classification of non-Newtonian models, that simulate blood behavior to different degrees of accuracy, there are many variants. The power law, Casson, Carreau and H-B models are the most popular non-Newtonian simulation models [4-9]. The bloodstream is sometimes modeled as a non-Newtonian core with a much less viscous Newtonian wall layer which is known as the two-fluid model [10]. The Casson model has been used to represent the steady flow of blood, *in vitro*, extending the fluid model with yield stress, shear-dependent viscosity, and a power law of one half, to the pulsatile flow in arterioles, venules, and capillaries. In the small vessels considered, inertial effects are negligible, pulsatile flow phenomena are quasi-steady, while viscous stress and pressure gradient forces experience an instantaneous balance. The plasma layer has a surprisingly large lubricating effect during periods when the effective shear viscosity is significantly higher than the ultimate high shear viscosity [4].

A mathematical model has been presented for periodic blood flow in a rigid circular tube of thin diameter [5]. Blood is presented as a 3-layered fluid by considering core fluid as a Casson fluid which is covered by a thin layer of Newtonian fluid (plasma). Taking into account the low and high shear rate behavior of blood, the appropriate parameters are empirically determined. Experimental fit results, for each non-Newtonian model, show the dependence of viscosity on the shear rate [6].

The power law, Casson and Carreau models are the most widely used simulation models giving various viscosity shear dependent functions. For a Newtonian fluid, the shear rate, γ, is considered high with constant viscosity of blood, $\eta = 0.035$ *Poise*.

Another two-fluid model with the suspension of all the erythrocytes in the core region as a non-Newtonian fluid and the plasma in the peripheral layer as a Newtonian fluid one, is represented by Sankar and Lee [4, 8, 10, 13]. The non-Newtonian fluid in the core region of the artery is represented by both Casson fluid and Herschel-Bulkley (H-B) fluid. It is noted that the plug-flow velocity, velocity distribution, and flow rate of the two-fluid H-B model are considerably higher than those of the two-fluid Casson model for a given set of parameters [10]. A velocity magnitude distribution of the grid cells shows that the Newtonian model is close dynamically to the Casson model while the power law model resembles the Carreau model [5]. Since the use of a power-law model to describe velocity profiles does not provide a consistent rheological description, Das et al. [9] used the Casson model, *in vitro*, on rat spinotrapezius muscle. Also, it is shown that the two-phase Casson model with a peripheral plasma layer is in quantitative agreement

with experimentally obtained velocity profiles in venules of rat muscle under low flow rate [8]. Chaturani and Samy [11] have mentioned that for tube diameter 0.095 mm blood behaves like H-B fluid rather than power-law and Bingham fluids. Iida [12] reports that velocity profile in the arterioles having diameter less than 0.1 mm are generally explained fairly by the two models. However, velocity profiles in the arterioles whose diameters are less than 0.065 mm do not conform to the Casson model but can still be explained by H-B fluid model. Moreover, H-B fluid model can be reduced to power-law fluid model when the yield stress is zero and Bingham fluid model when its power-law index n takes the value one. Thus, the two-fluid H-B model has more suitability than the two-fluid Casson model in the studies of blood flow through narrow arteries. For the two-fluid H-B model and the expressions for the flow quantities obtained by Sankar [13] for the two-fluid Casson model are used to compare these fluid models and bring out the advantage of using the two-fluid H-B model over two-fluid Casson model for blood flow in catheterized arteries. Non-Newtonian behavior also affects the wall shear stress predicting larger values than the Newtonian models [13-15].

Other mathematical models consider blood as a two-phase fluid, an RBC suspension in Newtonian incompressible plasma [16-18]. In this type of analysis, the RBCs are assumed to be rigid, neutrally buoyant spherical particles, and their specific gravity compared to that of plasma diminishes the effect of gravity on blood.

There is experimental evidence of the electric and magnetic fields effect on the haemodynamics of blood. International institutes have recorded maximum endurable dose of electric, magnetic and electromagnetic fields. The effects of commercial mobile phone signals, GSM, on various physiological processes have been the field of investigation and research for quite a while. These signals are proven to affect the cerebral blood flow in healthy humans using positron emission tomography (PET) imaging [19, 20]. The pulse modulated RF electromagnetic field, emitted by mobile phones is also proven to affect the EEG signals during sleep and wakefulness [21-23]. Continuous wave RF electromagnetic fields also affect cognitive performance [24]. Furthermore, EMF effects on microcirculatory system in different tissues in experimental animals are estimated in SAR for static magnetic field ranges of 0.3-180 mT [25].

For static magnetic fields, acute effects occur when there is movement in the field, such as motion of a person or internal body movement, such as blood flow or heart beat [26]. Static magnetic fields exert forces on moving charges in the blood, such as ions, generating electrical fields and currents around the heart and major blood vessels that can slightly impede the flow of blood. Possible effects range from minor changes in heartbeat to an increase in the abnormal heart rhythms, that might cause ventricular fibrillation [27]. These types of acute effects are only likely within fields in excess of 8 T.

To date, it is not possible to determine whether any long-term health consequences exist from exposure in the millitesla range because there are no well-conducted epidemiological or long-term animal studies. The recommended limits are time-weighted average of 200 mT during the working day for occupational exposure, with a ceiling value of 2T. A continuous exposure limit of 40 mT is given for the general public. Static magnetic fields affect implanted metallic devices such as pacemakers present inside the body, and this could have direct adverse health consequences. It is suggested that wearers of cardiac pacemakers, ferromagnetic implants like stainless steel stents and implanted electronic devices should avoid locations where the field exceeds 0.5 mT. EMF exposure, with ranges of 1.5-2 kV/m with frequencies of 1-100 GHz, can interfere with the proper operation of pacemakers. Also microwave exposure (1 mW/cm^2) are recorded to cause reversible nervous system disturbance and blood chemical alterations [28].

In the present study, we adopt a mathematical

simulation model to produce results representing the velocity profiles in axial and radial direction for a purely ionic fluid. The main aim of the model is to study the interaction of incident electric field, both dc and ac, with the ionic fluid. In this study, we consider ionic viscous steady Newtonian fluid that flows in a relatively large rigid cylindrical vessel under incident fields. For the sake of analogy to the blood flow simulation flow parameters follow the actual recorded blood data. If blood is assumed as a whole ionic fluid where the wall shear stress is considered to result in a relatively high shear rate, therein the present work is a close simulation. The flow is through a rigid large arterial section, where rouleaux is not likely to affect the flow. In addition blood flow is pulsatile because of the nature of the heart pumping actions which results in fluctuating pressure gradient. The pressure gradient applied follows the natural systolic-diastolic profile. These assumptions make computational and analytical effort more manageable

2. Model

In the present work, analysis of the ionic flow is aiming to be analogous to blood flow in large vessels. To implement this, two main assumptions are adopted. Firstly, the flow is considered to be Newtonian, though blood exhibits an evident non-Newtonian behavior especially in small blood vessels. The blood, being an anamolous fluid, can be represented by the famous two-fluid, Casson or H-B model [4-9]. On the other hand, for relatively large cylindrical vessels, the friction with walls becomes less effective. Hence the shear stress is assumed negligible. Also for high shear rates, as expected in a very large vessel, the most commonly used models nearly coincide giving constant viscosity coefficient value [6].

The choice of the Newtonian model is suitable for the assumption that the shear rate, γ (s^{-1}), in large blood vessels of radii r ($\geq$2 mm), is above 100 s^{-1} [7]. These models show differences within the range of less than 20% for shear rates higher than 150 s^{-1}. Secondly, the flow is assumed purely ionic. Furthermore, at low shear rates, that is, $\gamma < 100\ s^{-1}$, the *RBC*s aggregate and form what is known as rouleaux. Aggregation disperses as the shear rate increases, reducing the viscosity of blood. However, as the shear rate increases, the shear-thinning characteristics disappear and blood demonstrates a Newtonian behavior [8].

3. Mathematical Analysis

The present work assumes a Newtonian incompressible ionic fluid flowing with velocity $v = (v_r, 0, v_z)$, in a cylindrical section shown in Fig. 1. We start with the Navier-Stokes equation:

$$\rho \frac{D\mathbf{v}}{Dt} = -\nabla p + F + \nabla \times [\eta(\nabla \times \mathbf{v})] + \nabla[\nabla . \mathbf{v}] \quad (1)$$

where ρ is the mass density, η is the viscosity coefficient, ∇p the pressure gradient and F is the body force. For incompressible fluids the continuity equation; $\nabla . v = 0$, is satisfied, hence:

$$\rho \frac{D\mathbf{v}}{Dt} = -\nabla p + F + \nabla \times [\eta(\nabla \times v)] \quad (2)$$

Adopting the Newtonian Model, the viscosity being constant and shear independent, as mentioned above, hence:

$$\rho \frac{Dv}{Dt} = -\nabla p + F + \eta \nabla^2 v \quad (3)$$

To produce a time varying velocity distribution along the axis and across the radius, the cylindrical coordinates would be suitable to work with.

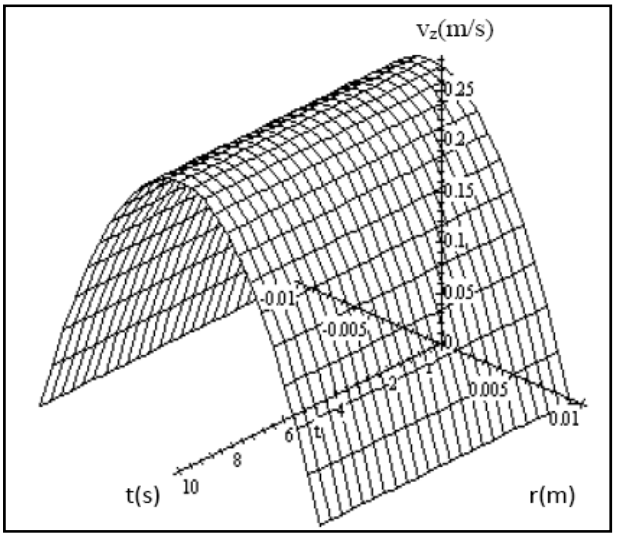

Fig. 1 Axial velocity versus both time and radius under zero incident field.

$$\rho \frac{\partial \mathbf{v}}{\partial t} = -\frac{\partial p}{\partial z} + F + \eta \left[\frac{\partial^2 \mathbf{v}}{\partial r^2} + \frac{1}{r}\frac{\partial \mathbf{v}}{\partial r}\right] \quad (4)$$

Boundary condition to be satisfied is the no slip boundary condition for the velocity z-component; $v_z = 0$ at $r = R$, is applied to the cylindrical flow. Besides, the symmetry about z-axis imposes the condition; $\frac{\partial \mathbf{v}}{\partial r} = 0$ at $r = 0$. While adopting the Poiseulle parabolic flow profile as a radial distribution, Eq. (4) is solved, imposing zero initial condition. The velocity in the z-direction varies with time, t, and radius, r, as follows:

$$v_z(r,t) = \frac{f_0(t)}{4}(R^2 - r^2)\left(e^{-\frac{4t}{\rho(R^2-r^2)}} - 1\right) \quad (5)$$

The function $f_0(t)$ represents the driving force:

$$f_0(t) = \frac{1}{\eta}\left(\frac{\partial p}{\partial z} - F_z\right) \quad (6)$$

3.1 Hydroelectric Flow

An incident axial electric field assumed to be applied, $\underline{E_{inc}} = (0, 0, E_z)$. This field essentially induces a magnetic field that circulates in the x-y plane, $B_{ind} = (0, B_\theta, 0)$. For the hydroelectric flow under investigation, the body force, F_z, is expressed as electric and magnetic body forces due to the incident and induced fields. If the volumetric ionic charge density is $\pm\rho_e$, hence;

$$F_z = \rho_e (E_z + v_r B_\theta) \quad (7)$$

Originally, the current density vector for the flow of positive charges in the axial direction and equals:

$$J_z = 1.6 \times 10^{-19} \times \rho_e \times v_z \quad (8)$$

An axial current density, J_z , is generated due to the incident electric and induced magnetic fields:

$$J_z = \sigma(E_z + v_r \cdot B_\theta) \quad (9)$$

where σ is the electrical conductivity of the fluid.

Hence, a radial force component, F_r, is generated; $F_r = J_z \cdot B_\theta$

3.2 Hydroelectric Capacitance

An instantaneous capacitance is created due to the separation of the positive and negative ions that move along the axis with different velocities. The value of the cross sectional capacitor created after a time interval, Δt (s) is:

$$C(t) = \frac{\varepsilon \pi R^2}{(v^+(t) - v^-(t))\Delta t} \quad (10)$$

where $v^+(t)$ and $v^-(t)$ are the axial velocities when the ionic concentration is inserted in Eq. (6) as ρ_{e+} or ρ_{e-} respectively, and ε is the permittivity of the ionic fluid. Furthermore, the radial force component, F_r, acts on the positive and negative ions in opposite directions creating a time dependent cylindrical capacitor.

4. Results

For the sake of analogy with the blood flow in a large arterial vessel, the parameters used here are those reported for blood. The concentration of different ions in plasma is given in Ref. [7]. The blood plasma can be considered as a two-fluid ionic solution one of positive electric charge concentration ρ_{e+} and another of negative charge concentration ρ_{e-} To simulate the blood flow in a large arterial-like section of radius, R = 1 cm, average reported parameters for plasma are as given below [4-7]: ρ = 1,030 kg/m^3, η = 0.0035 kgm^{-1}s^{-1} , $\rho_{e-} = 0.1269$ c/m^3, $\rho_{e+} = 0.1407$ c/m^3

The axial velocity, v_z (m/s), is represented against time, t (s) for different radii values, r (m). Fig. 1 shows the three dimensional representation of the axial velocity versus both time and radius without any external field under a constant pressure gradient of, $\frac{\partial p}{\partial z}$ = -40 Pa/m. It shows a parabolic distribution of maximum 0.25 m/s hence delivering a volumetric rate of 5.2 l/s.

4.1 The Flow under Constant Pressure Gradient

The effect of the exposure to an electric field incident along the axial flow is investigated. Firstly, the pressure gradient is assumed constant throughout the arterial section having the same pressure gradient value as above. The axial electric field, E_z, is applied as a steady dc field and varied from 100 V/m to 0.35 kV/m. The axial velocity v_z is represented against time and radius in Fig. 2, for incident electric field 100 V/m. While Fig. 3 shows the velocity distribution for an

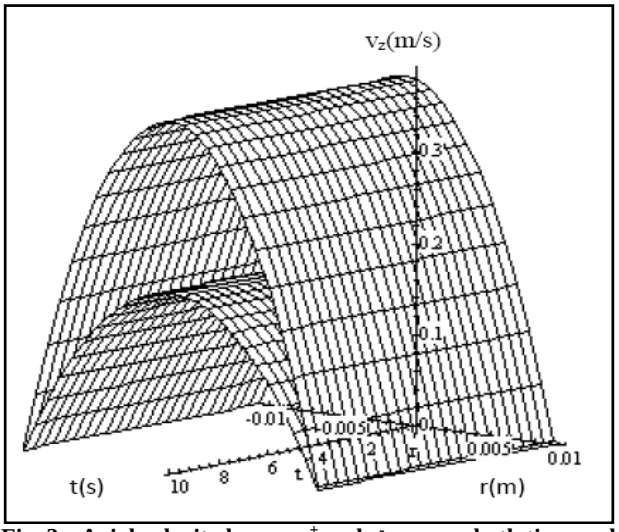

Fig. 2 Axial velocity layers, v^+ and v^-, versus both time and radius under 100 V/m incident field.

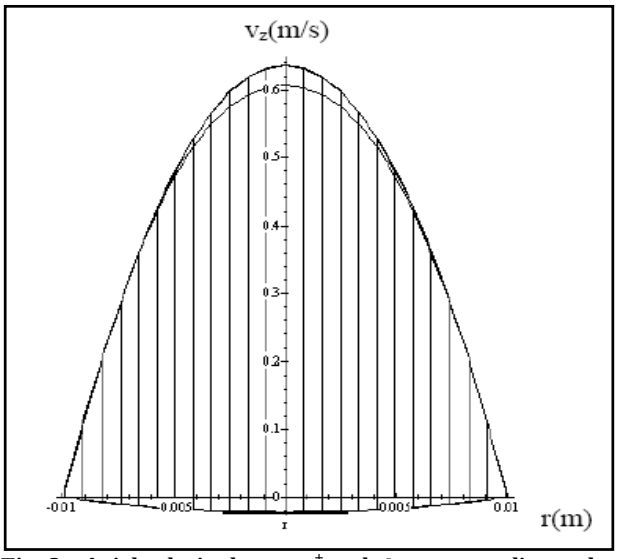

Fig. 3 Axial velocity layers, v^+ and v^-, versus radius under 350 V/m incident field.

incident field of 350 kV/m against the cylindrical radius.

The axial velocity is represented for both positive and negative ionic distribution. The separation of the fluid layers is obvious in Fig. 2.

A force, acts in positive z-direction, on ρ_{e+}, produces v^+ of maximum 0.32 m/s, whereas an opposing one acts on ρ_{e-}, produces v^- of maximum 0.189 m/s. At a threshold electric field value of 0.31 kV/m, the negatively charged ionic fluid layer starts to reverse its direction. As Fig. 3 shows the reversing of the negatively charged ionic layer under the effect of an incident electric field 350 V/m, where v^-_{max}= *-0.02* m/s and v^+_{max} = 0.64 m/s.

4.2 The Flow under Pulsating Pressure Gradient and DC Electric Field

Secondly, for simplicity the pressure gradient is assumed to be pulsating in sinusoidal manner with periodicity *T*. In this case, the pressure gradient takes a mathematical expression to simulate as much as possible the natural biphasic waveform of heart beat. The pressure is assumed a fluctuating function of periodicity, T = 750 ms:

$$\frac{dp}{dz} = -40\, sin\left(2\pi \frac{t}{T}\right) \qquad (11)$$

Under these conditions three different cases are studied. Namely, the effect of applying dc electric field along the axis, with constant values of: 10 V/m, 100 V/m, 250 V/m. The velocity waveforms for the positive ionic layer, $v^+_z(r,t)$, are shown in Fig. 4. The root mean square velocity values, V^+_{rms} are 0.200914 m/s, 0.22157 m/s and 0.31304 m/s, respectively.

4.3 The Flow under Pulsating Pressure Gradient and AC Electric Field

The effect of applying AC electric field in the cylindrical section along the axial direction is studied. In this case, the electric field takes the sinusoidal form of $E_z = E_0 \sin(2\pi ft)$.

Thus the induced magnetic field is: $B_\theta = \sqrt{\varepsilon\mu}\, E_0 \cos(2\pi ft)$, where ε is the permittivity of the ionic fluid assumed as 0.2656×10^{-10} F/m, μ is its magnetic permeabilitiy, 1.2547×10^{-6} H/m and f is the frequency of the field. For E_0 = 100 V/m and frequency 50 Hz, the simulated velocity waveform, $v_z(r,t)$, is as shown in Fig. 5.

It is obvious that the velocity profile exhibits a complex waveform that includes both the pressure wave frequency together with that of the incident electric field besides other harmonics.

For different values of the frequency, *f*, namely: 50 Hz, 1 kHz, 1 MHz and 1 GHz, the positive ionic layer waveform is represented in Fig. 6. Harmonics for the

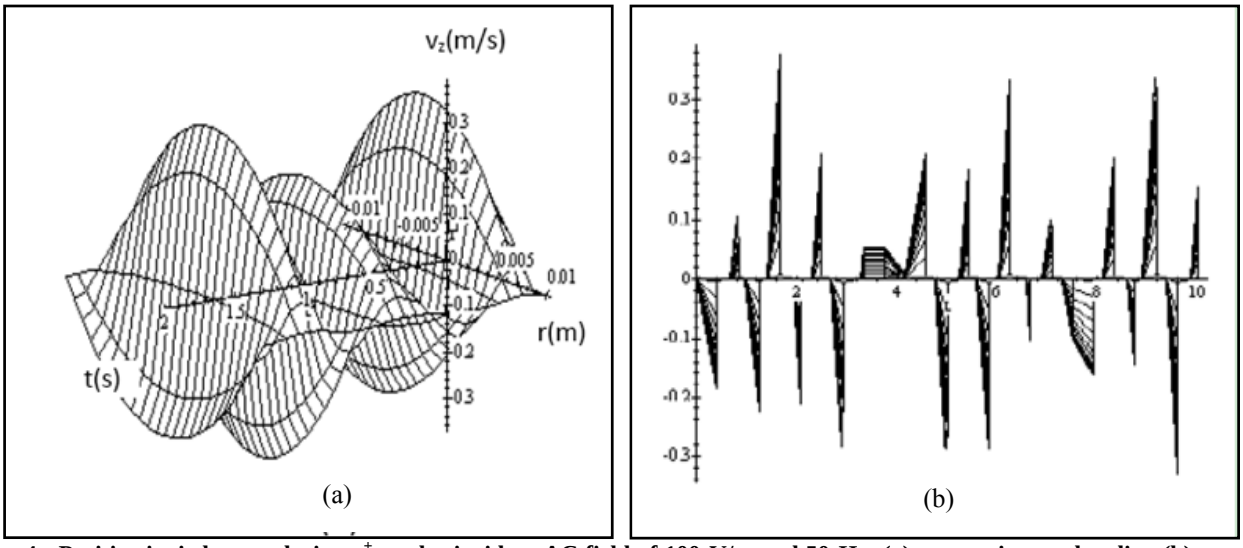

Fig. 4 Positive ionic layer velocity, v^+, under incident AC field of 100 V/m and 50 Hz: (a) versus time and radius (b) versus time.

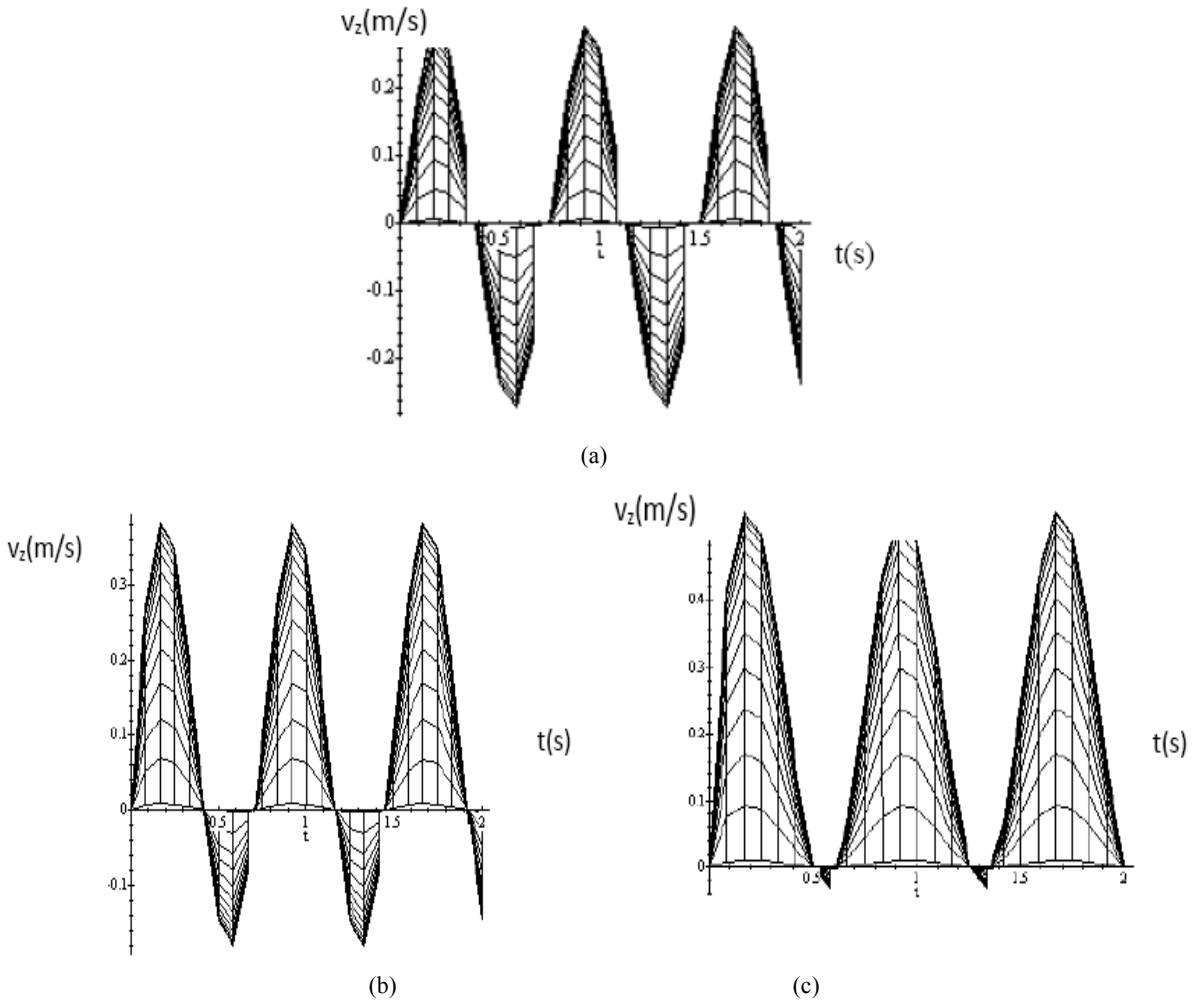

Fig. 5 Axial positive layer velocity, v^+, versus both time under incident fields: (a) E_0 = 10 V/m (b) E_0 = 100 V/m (c) E_0 = 250 V/m.

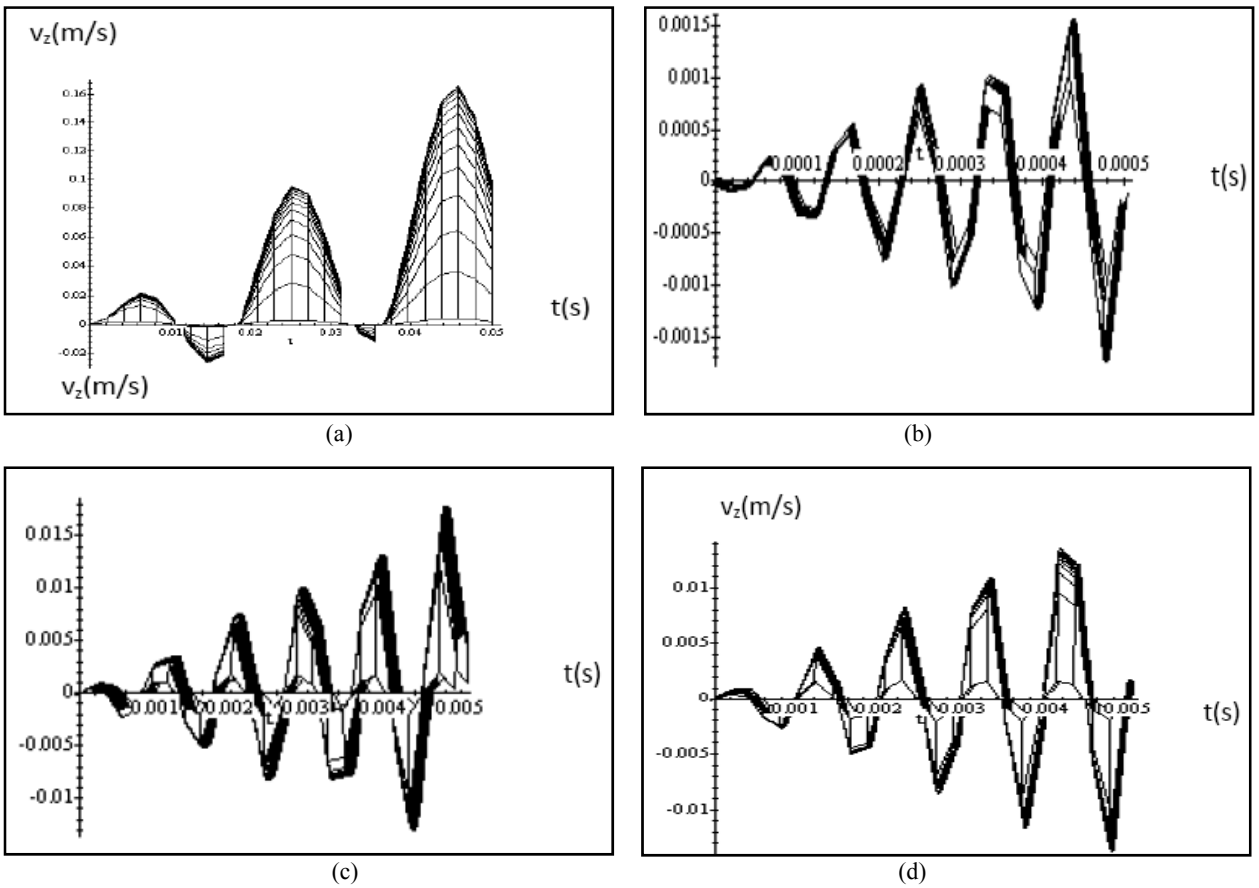

Fig. 6 Axial positive layer velocity, v^+, under incident field: 100 V/m and 50 Hz: (a) f = 50 Hz (b) f = 1 kHz (c) f = 1 MHz (d) f = 1 GHz.

different cases are evident while the time axis scale is enlarged to give a closer view.

The root mean square values of the axial velocity component for both positive and negative ionic layers are calculated for different values of DC and AC field strengths. It is worthwhile to note that beyond the threshold DC electric field strength value given above, namely 330 V/m, the velocity distributions of ionic layers exhibit a 180˚ phase shift. These values are given in Table 1, together with the Reynold's number.

Furthermore, the power density, S_r, is calculated as the rms value of, $E_z B_\theta$. The power density, in mw/m^2, is calculated as S_r/μ. It is time variant, dependent on the incident field parameters and dissipated through the radial direction.

5. Discussion

Table 1 shows that under the given conditions, Reynold's number is below the turbulent flow value which justifies the adopted Newtonian approach. This is the case for different ranges of electric fields applied at different frequencies up 1 GHz. Also it applies to both types of ions. For constant ac electric field strength of 100 V/m, the Reynold's number shows consistency though the frequency changes from 1 kHz up to 1 GHz. This indicates that the steadiness of flow is not affected by the change in frequency. And consequently the velocities of both positive and negative ionic layers are unaffected. Electric field strength shows a threshold of 350 V/m where Reynold's number is critical and turbulence can occur at any slight increase of the field.

It is noteworthy to point out that the associated magnetic field creates forces on the positively charged particles radial inward while the negatively charged particles experience outward radial forces. This may

Table 1 Flow variables.

f (kHz)	E_0 (V/m)	$B_0\times10^{-2}$ (mT)	V^{+}_{rms} (m/s)	V^{-}_{rms} (m/s)	Re^{+}	Re^{-}	S_r (mVT/m)
0	100	0.0577	0.17	0.1	503.52	294.29	0.05773
0	200	0.1155	0.22	0.04	676.85	117.71	0.2310
0	300	0.1732	0.27	0.01	794.57	29.4	0.5196
0	350	0.2021	0.32	0.01	940.83	29.4	0.7073
1	100	0.0577	0.21	0.21	625.12	578.12	0.0204
1	200	0.1155	0.24	0.24	717.44	690.28	0.0817
1	300	0.1732	0.29	0.27	849.31	797.05	0.1837
1	350	0.2021	0.31	0.29	924.99	859.36	0.2501
10^3	100	0.0577	0.21	0.21	625.12	578.12	0.0204
10^6	100	0.0577	0.21	0.21	625.12	578.12	0.0204

lead to charge separation along the radial direction. Under a certain value of the magnetic field one can speculate that the positive ions would coincide with the axis while the negative ions stick to the inner wall.

Another time dependent capacitance appears axially along the flow due to the formation of oppositely charged disc-like ionic layers expressed as in Eq. (10) and illustrated in Fig. 2 for the DC field case.

6. Conclusions

The ultimate purpose of the present investigation is to study the effect of external electric field on the blood flow. Therefore we are keen to use as much as possible and available, the reported physical data concerning human blood. There are two major obstacles in building up a model of blood flow namely vessel viscoelasticity and non circular irregular vessel cross section. However this work introduces a simplified approach to the problem. Hence we establish a strong correlation between incident axial electric field and velocity profiles under different conditions.

Reference

[1] M.A. El-Naggar, M.A. El-Messiery, The viscoelastic response of blood vessels under the effect of pulsatile pressure, in: proc. of the 3rd international workshop on the biological effects of electromagnetic fields, Kos, Greece, 2004, pp. 50-55.

[2] M.A. El-Naggar, A double layer arterial wall model under pulsating blood pressure, in: Proc. of the 4th international workshop on the biological effects of electromagnetic fields, Crete, Greece, 2006, pp. 1412-1418.

[3] M.A. El-Naggar, An investigation on silicone and silicone rubber stents in comparison with stainless steel stents, in: Proc. of the 5th international workshop on the biological effects of electromagnetic fields, Terrasini, Palermo, Italy, 2008.

[4] D.S. Sankar, U. Lee, Pulsatile flow of two-fluid nonlinear models for blood flow through catheterized arteries: A comparative study, Journal of Mechanical Science and Technology 23 (9) (2010) 2444-2455.

[5] R.P. Maurya, H. Khas, Peripheral layer viscosity effects on periodic blood flow through rigid tube of thin diameter, Journal of Mathematical Analysis and Applications 124 (1987) 43-51.

[6] J. Aroesty, J.F. Gross, Pulsatile flow in small blood vessels, Mathematical Problems in Engineering (2010) 21.

[7] S.S. Shibeshi, W.E. Collins, The rheology of blood flow in a branched arterial system, Appl Rheol. 15 (6) (2005) 398-405.

[8] D.S. Sankar, U. Lee, An open access article distributed under the Creative Commons Attribution License, Clin Hemorheol Microcirc 36 (3) (2007) 217-233.

[9] B. Das, J.J. Bishop, S. Kim, H.J. Meiselman, P.C. Johnson, A.S. Popel, Red blood cell velocity profiles in skeletal muscle venules at low flow rates are described by the Casson model, Center for Scientific Computation and Mathematical Modeling, Univ. of Maryland, College Park, MD 20742, USA.

[10] D.S. Sankar, A. Izani, M. Ismail, Two-fluid mathematical models for blood flow in stenosed arteries: A comparative study, School of Math. Sciences, Univ. of Science, 11800 Penang, Malaysia, Jan. , 2009.

[11] P. Chaturani, V.R.P. Samy, A study of non-Newtonian aspects of blood flow stenosed arteries and its applications in arterial diseases, Biorheology 22 (6) (1985) 521-531.

[12] N. Iida, Influence of plasma layer on steady blood flow in microvessels, Japanese Journal of Applied Physics 17 (1978) 203-214.

[13] D.S. Sankar, U. Lee, Two-phase non-linear model for the

flow through stenosed blood vessels, Journal of Mechanical Science and Technology 21 (4) (2007) 678-689.

[14] D.S. Sankar, K. Hemalatha, Pulsatile flow of Herschel-Bulkley fluid through stenosed arteries: A mathematical model, International Journal of Non-linear Mechanics 41 (8) (2006) 979-990.

[15] D.S. Sankar, J. Goh, A.I.M. Ismail, FDM analysis for blood flow through stenosed tapered arteries, Boundary Value Problems 2010 (2010) 917067.

[16] R. Usha, K. Prema, Pulsatile flow of particle-fluid suspension model of blood under periodic body acceleration, Zeitschrift für Angewandte Mathematik und Physik (ZAMP) 50 (2) (1999) 175-192.

[17] A.W. Isaac, M. Mathuieu, A mathematical model for blood flow under periodic acceleration, Proceedings of the English IASTED International Conference on Biomedical engineering, BioMed 2011, Innsbruck, Austria, Feb., 2011.

[18] A.W. Isaac, Calculation of the pressure gradient, velocity and wall shear in arteries for a given flow rate, International Journal of Eng. Science, NANO-11-1008, 2010.

[19] R. Huber, Exposure to pulse modulated radio frequency electromagnetic fields affects regional cerebral blood flow, Eur. J. Neurosci 21 (2005) 1000-1006.

[20] S. Aalto, Mobile phone affects cerebral blood flow in humans, Journal of Cerebral Blood Flow and Metabolism 26 (2006) 885-890.

[21] A.A. Borely, Pulsed high frequency electromagnetic field affects human sleep and sleep electroencephalogram, Neurosci Letters 275 (1999) 207-210.

[22] R. Huber, Exposure to pulsed high-frequency electromagnetic fields during waking affects human sleep EEG, Neuro. Report 11, 2000, pp. 3321-3325.

[23] R. Huber, Radio frequency electromagnetic field exposure in humans: Estimation of SAR distribution in the brain, effects on sleep and heart rate, Bioelectromagnetics 24 (2003) 262-276.

[24] S.J. Regel, Effects of pulsed and continuous-wave radio frequency electromagnetic fields on cognitive performance and the waking EEG, NeuroReport 18 (2007) 803-807.

[25] C. Ohkubu, EMF effects on microcirculatory system, Springer Science & Business Media LLC, 2007.

[26] S.Y. Sekino, Biological effects of electromagnetic fields and recently updated safety guidelines for strong static magnetic fields, Magnetic Resonance in Medical Sciences 10 (2011) 1-10.

[27] International Commission on Non -Ionizing Radiation Protection, IARC, 2002, Internet communication, www.icnirp.org.

[28] G. Baker, Summary of the Effects of EMF Radiation, Safety, Health and Environment, 2009.